



UNIVERSITY OF LEEDS

This is a repository copy of *Characterisation of the surface topography, tomography and chemistry of fretting corrosion product found on retrieved polished femoral stems*.

White Rose Research Online URL for this paper:
<https://eprints.whiterose.ac.uk/80860/>

Version: Accepted Version

Article:

Bryant, M orcid.org/0000-0003-4442-5169, Ward, M, Farrar, R et al. (4 more authors) (2014) Characterisation of the surface topography, tomography and chemistry of fretting corrosion product found on retrieved polished femoral stems. *Journal of the Mechanical Behavior of Biomedical Materials*, 32. pp. 321-334. ISSN 1751-6161

<https://doi.org/10.1016/j.jmbbm.2013.11.016>

Reuse

Items deposited in White Rose Research Online are protected by copyright, with all rights reserved unless indicated otherwise. They may be downloaded and/or printed for private study, or other acts as permitted by national copyright laws. The publisher or other rights holders may allow further reproduction and re-use of the full text version. This is indicated by the licence information on the White Rose Research Online record for the item.

Takedown

If you consider content in White Rose Research Online to be in breach of UK law, please notify us by emailing eprints@whiterose.ac.uk including the URL of the record and the reason for the withdrawal request.



eprints@whiterose.ac.uk
<https://eprints.whiterose.ac.uk/>

**CHARACTERISATION OF THE SURFACE TOPOGRAPHY, TOMOGRAPHY AND
CHEMISTRY OF FRETTING CORROSION PRODUCT FOUND ON RETRIEVED
POLISHED FEMORAL STEMS**

M.Bryant^a, M. Ward^b, R. Farrar^c, R. Freeman^c, K. Brummitt^c, J. Nolan^d, A. Neville^a

a – Institute of Engineering Thermofluids, Surfaces and Interfaces (iETSI), School of Mechanical Engineering, University of Leeds, Leeds, LS2 9JT, United Kingdom .

b – Institute of Materials Research (IMR), School of Engineering, University of Leeds, Leeds, LS2 9JT, United Kingdom.

c – DePuy International, Millshaw Park Lane, Leeds, LS11 0BG. United Kingdom.

d – Norfolk and Norwich University Hospital, Norwich, United Kingdom.

CORRESPONDING AUTHOR:

Mr. M. Bryant (m.g.bryant@leeds.ac.uk)

Institute of Engineering Thermofluids, Surfaces and Interfaces (iETSI), School of Mechanical Engineering, University of Leeds, Leeds, LS2 9JT, United Kingdom.

Tel: +44 (0)113 3432215

HIGHLIGHTS:

- The tomography of retrieved femoral stems was characterised.
- Directionality and plastic deformation of the metallic surfaces was seen.
- Thick deposited layers were seen to occur within the stem-cement interfaces.
- Films of Cr_2O_3 bound with organic material play an important role in the degradation.
- Tribocorrosion and tribochemical reactions affect the quantity of ions produced.

Abstract

This study presents the characterisation of the surface topography, tomography and chemistry of fretting corrosion product found on retrieved polished femoral stems. Scanning Electron Microscopy (SEM), X-ray Photoelectron Spectroscopy (XPS), Transmission Electron Microscopy (TEM) and Fourier Transform Infrared Spectroscopy (FTIR) were utilised in order to assess the surface morphology of retrieved Metal-on-Metal Total Hip Replacements and surface chemistry of the films found on the surface. Gross slip, plastic deformation and directionality of the surface were extensively seen on the proximal surfaces of the retrievals. A more corrosive phenomenon was observed in the distal regions of the stem, demonstrating a seemingly intergranular attack. Tribochemical reactions were seen to occur within the stem-cement interfaces with tribo-films being observed on the femoral stem and counterpart PMMA bone cement. XPS, TEM-EDX and FTIR analysis demonstrated that the films present in the stem surfaces were a complex mixture of chromium oxide and amorphous organic material. A comparison between current experimental and clinical literature has been conducted and findings from this study demonstrate that the formation and chemistry of films are drastically influenced by the type of wear or degradation mechanism. Films formed in the stem-cement interface are thought to further influence the biological environment outside the stem-cement interface due to the formation of Cr and O rich films within the interface whilst Co is free to migrate away.

1. Introduction

The method of using artificial devices to replace joints has been a method practised since the late nineteenth century by Gluck (Feng and Barrans, 1956; Reynolds and Tansey, 2006). However it has only recently become a long term solution to arthritic and congenital diseased joints since the 1950's due to the advances in both fixation technique and implant design made by Sir John Charnley. The orthopaedics industries have made many advances since and Total Hip Arthroplasty (THA) is now widely accepted as being a successful surgical procedure with results from the National Joint Registry supporting this (National Joint Registry, 2012). THA's are commonly used to treat arthritis or severe joint damage. Osteoarthritis of the hip joint is a painful and debilitating condition, estimated to affect 8 million people in the United Kingdom and 27 million in the United States (National Joint Registry, 2012; World Health Organisation, 2003). Different treatments exist but to date the most effective method of alleviating pain and restoring motion is THA. THAs are also used to mitigate other forms of hip disease such as rheumatoid arthritis, traumatic arthritis, hip fractures and tumours.

MoM Total Hip Replacements (THR) have the longest clinical history of any of the bearing combinations with the first generation of MoM THR being designed and developed by Philip Wiles in 1938. However these implants were largely unsuccessful due to the poor quality of material which was primarily stainless steel, poor manufacture and lack of inadequate fixation within the body. MoM THR's regained popularity due to improved manufacturing methods and decreased wear rates. Retrieval studies indicate that well-functioning MoM THR's produce minimal wear debris and the surrounding tissues appear to have less inflammation compared with typical histiocyte-dominated tissue response to polyethylene debris. However in the recent years the amount of revisions has increased due to the Adverse Reaction to Metal Debris (ARMD) (National Joint Registry, 2012).

The United Kingdom's National Joint Registry indicates that in 2011, 71,672 primary hip procedures were conducted. Of the 71,672 primary hip procedures undertaken in 2011, of which 36% were cemented total hip replacements representing a significant proportion of implants on the NHS. Although the method of cementing the femoral component is a well-established technique, yielding superior short term results, an increasing trend away for the cemented technique to cementless fixation has been seen. In 2008, Donell et al (Donell et al., 2010) reported the dramatic fretting-corrosion of generally solidly fixed femoral stems when combined with MoM articulations. It was thought that the necrosis of the surrounding tissue was associated with the release of potentially toxic metal ions such as cobalt and chromium from the stem-cement interface due to corrosion of the alloy. A subsequent publication by Boland et al (Bolland et al., 2011) in 2011 further demonstrated levels of corrosion of the with cemented MoM devices further highlighting that the degradation mechanisms at the stem-cement interface can have serious implications. Unfortunately, the early failure of THA's has attracted substantial press attention, with the suitability of MoM implants and the metal ion release associated with such implants being questioned by many experts and the tabloid press.

Biomedical alloys typically owe their corrosion resistance to the formation of an inert protective oxide film resulting in very low corrosion rates. In order for a material to form a passive film, the substrate must rapidly react with oxidising agents in the environment. When a passive alloy is utilised in tribological application, depending on the contact mechanics and lubrication regimes, mechanical removal of the passive film occurs leaving the reactive substrate exposed to the environments free to oxidise or corrode (Mischler, 2003). This is known as tribocorrosion. It is universally agreed that biomedical implants are subjected to sliding tribocorrosion at the articulation (large amplitudes of sliding >20mm) and fretting-corrosion at the modular taper and stem-cement interfaces (small

amplitudes of sliding <250µm). It is also important to appreciate that MoM THR's are electrically coupled via their interfaces, as well as across the metallic surface, resulting in numerous galvanic cells been established. Tribochemistry is a branch of chemistry dealing with the chemical and physiochemical changes of matter due to the influence of mechanical energy (Muratov et al., 1998). The tribochemical reactions occurring on orthopaedic implants have been recognised as an important factor when considering the longevity of implants. Figure 1 summarises the possible locations and mechanisms for tribocorrosion and tribochemical reactions to occur.

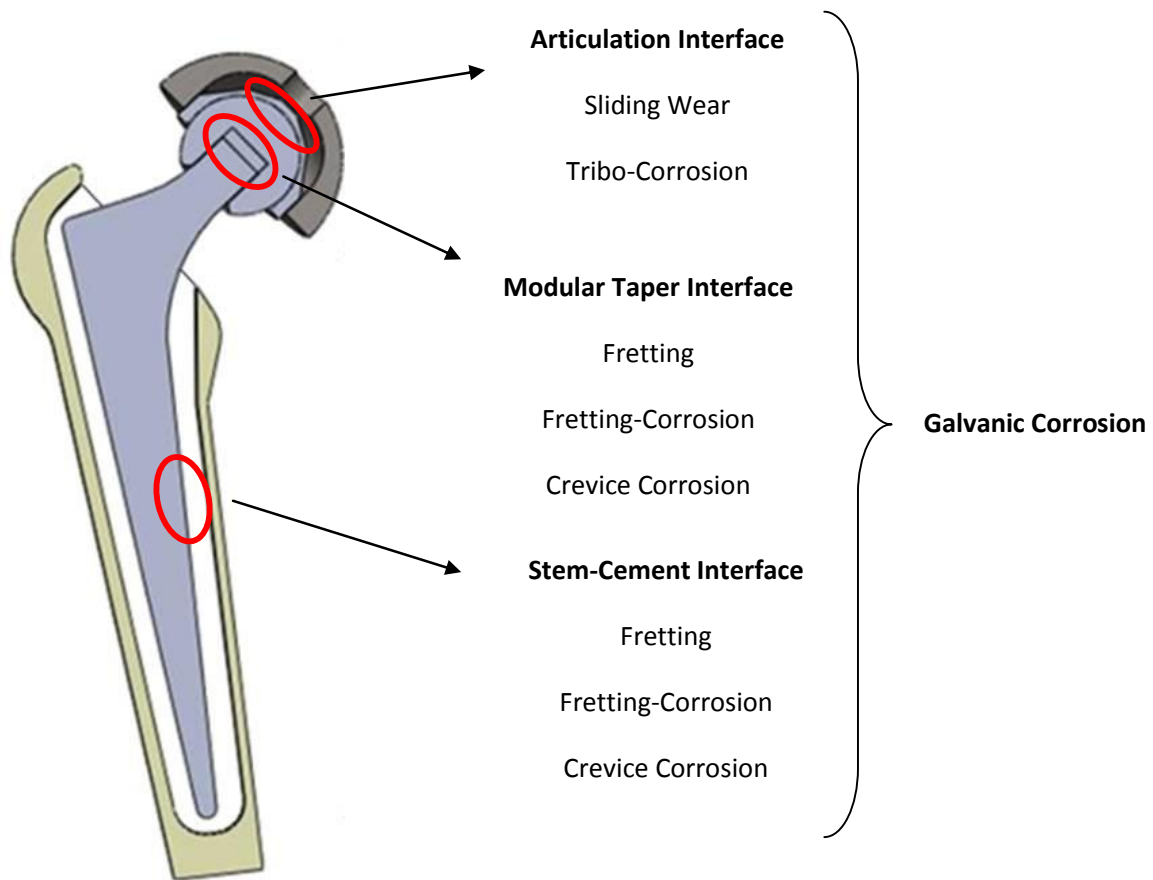


Figure 1 – A schematical representation of a THR with the associated tribo-corrosion mechanisms.

To date the authors have presented experimental and preliminary clinical finding outlining the mechanisms, system variables influencing the degradation and the elemental chemistry of both laboratory simulated and retrieved CoCrMo femoral stems (Bryant et al., 2013a; Bryant et al.,

2013b; Bryant et al., 2013c). The aim of this study was to further understand and characterise the exact surface chemistry, speciation and tribochemical reactions resulting in the deposits observed on retrieved femoral components; an unappreciated area of study with respect to the degradation and type of debris generated from orthopaedic implants. A comparison between deposits produced in-vivo and experimentally, along with a comparison of literature relating to tribochemical reactions has been made. Advanced surface analysis techniques have been employed in order to evaluate the surface and subsurface characteristics of retrieved LC CoCrMo femoral stems. Due to the advances in surface analysis techniques and a more in-depth understanding of the tribological and tribocorrosion at the nano-scale, this study also aims to compare and contrast current literature regarding the formation of tribo-films associated with orthopaedic implants.

2. Materials and Method

The Implant: The Ultima TPS™ (DePuy International, Leeds) hip replacement system was one of the first second-generation MoM hip replacement to be developed consisting of a collarless, tapered, highly polished wrought low carbon (LC) CoCrMo femoral stem with a 12/14 modular taper. A 28mm MoM articulation was utilised in this cohort consisting of a wrought LC CoCrMo Ultima femoral head and a wrought high carbon (HC) CoCrMo taper lock acetabular insert. A porous coated Ti-6Al-4V Acetabular outer shell with three holes for supplementary fixation was used. Figure 2 demonstrates the system that was implanted in the cases presented by Donell et al (Donell et al., 2010).

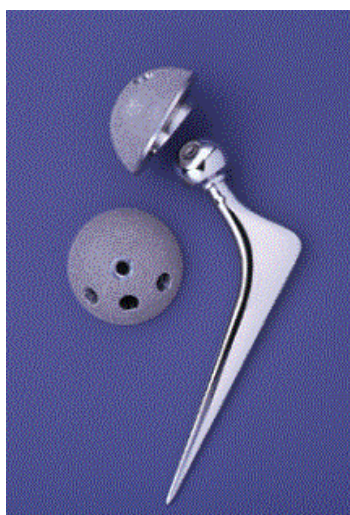


Figure 2 – Ulitma TPS™ MoM total hip replacement used in the Norwich cohort

Retrieved Cohort and Analysis Details: Between 1997-2008, 90 out of a total series of 652 Ultima TPS™ hip replacement systems metal-on-metal hip replacements had to undergo early revision at the Norfolk and Norwich University Hospital. 17 hips required revision for periprosthetic fracture, with early dislocation in 3 and late dislocations in 16. Infection was found in 10 hips. 44 required revision for extensive, symptomatic, peri-articular soft tissue necrosis of which 35 had normal plain radiographs. The femoral component was cemented with either a plain PMMA bone cement or antibiotic cement containing either the Gentamicin antibiotic or Erythromycin and Colistin. Dramatic corrosion of generally solidly fixed femoral stems was frequently observed on the retrieved cemented part of the femoral component. Blackening of the cemented portions of the stems and staining of the PMMA bone cement, thought to be metallic debris, was also found at revision. It was thought that the necrosis of the surrounding tissue was associated with the release of potentially toxic metal ions such as cobalt and chromium from the stem surface as the bearing surfaces were macroscopically clean of any wear or abrasion. A Medical Device Alert MDA/2007/054 dated 14 June 2007 was issued detailing unexplained pain when the Ultima TPS femoral stem was used in conjunction with the 28mm Ultima MoM articulation. As of 2012, 132 revisions from 652 hips have been conducted with two thirds of revisions been symptomatic of Adverse Reaction to Metal Debris (ARMD).

In this study, 105 Ultima TPS MoM THR were retrieved from the Norfolk and Norwich teaching hospital. Each stem underwent a sterilisation wash procedure before the analysis was undertaken. Each implant was individually placed in a cardboard surgical tray, sealed in a polythene bag and numbered in numerical order to ensure patient data was kept confidential. Any handling of the implants was performed using latex surgical gloves to avoid contamination.

Prior to microscopic observations, each THR was sectioned according to Gruen et al (Gruen et al., 2011) and macroscopically graded in terms of fretting-corrosion and location and have been reported previously (Bryant et al., 2013d). After macroscopic analysis a select number of stems were sectioned and Scanning Electron Microscopy (SEM) with integrated Energy Dispersive X-ray (EDX) spectroscopy was conducted using a Carl Zeiss EVO MA15 microscope in order to inspect the stem surfaces at a higher resolution and to gain a basic elemental composition of any debris or deposits found on the surface of the stem.

Focused Ion Beam (FIB) sample preparation and subsequent TEM was also utilised as a technique to quantify the exact composition, thickness and morphology of any deposit or corrosion product. To

achieve this, an area of interest was identified on the stem and a TEM section was prepared for analysis using a FEI Nova200 Nanolab dual beam SEM/FIB. In order to do this, an initial layer of Pt ($\approx 200\text{--}300\text{nm}$) was deposited using an electron beam in order to protect to the surface during preparation (Figure 3b). A second layer of Pt, $1.5\ \mu\text{m}$ thick, was then deposited on top of the initial Pt layer using the Ga^+ ion beam (Figure 3c). Once this was complete material either side of the deposited Pt layer was milled away to an approximate depth of $10\ \mu\text{m}$ using the ion beam (Figure 3d). Further thinning of the section was then performed, and the section was partially cut free from the bulk material (Figure 3e). It was then removed using a Kleindiek micromanipulator mounted inside the chamber of the microscope and attached to a Cu TEM grid, secured via Pt deposition (Figures 3f-g). The attached sample was further milled using the FIB in order to reduce the thickness of the samples. This was until a thickness of $<100\ \text{nm}$ was achieved, meaning the sample was electron transparent (Figure 3h). The sample was then placed in a FEI Tecnai F20 FEGTEM fitted with an Oxford Instruments X-max SDD EDX detector for TEM analysis.

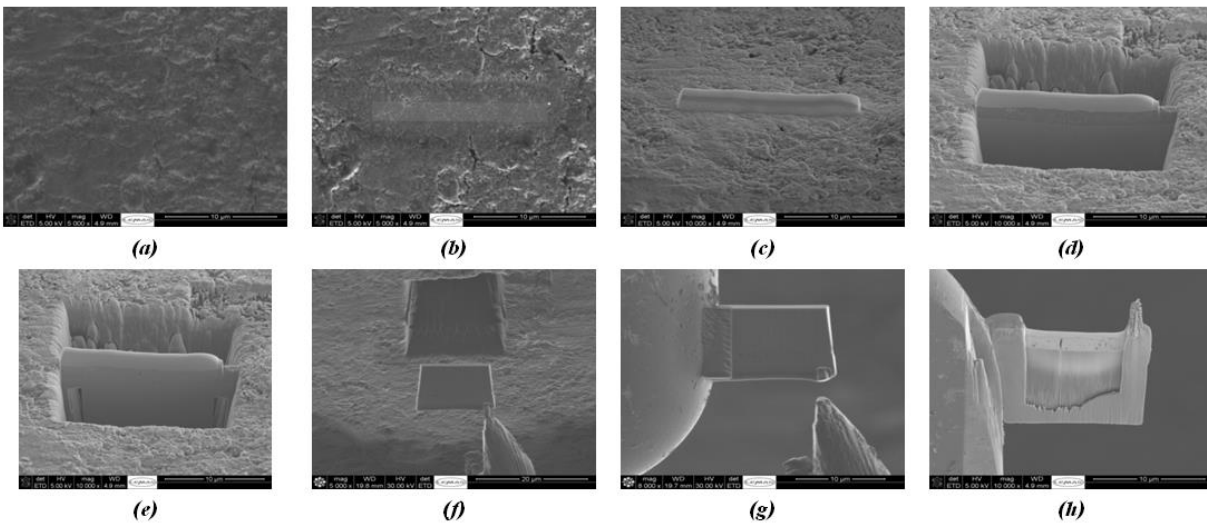


Figure 3 – FIB SEM preparation of TEM section (a) surface prior to Pt deposition (b) electron deposited Pt layer (c) ion deposited layer (d) bulk removal of material either side of the section (e) cutting the section free prior to removal (f) removal of the section (g) fixation of FIB prepared section to Cu TEM grid and (h) final thinning of the prepared section.

X-ray photoelectron spectroscopy (XPS) was further utilised to establish the exact chemical composition of any debris or deposit found on the surface. XPS analysis was carried out using a VG Escalab 250 with a high intensity monochromatic Al $\text{K}\alpha$ X-ray source (1486.6eV) with a lateral resolution of $500\ \mu\text{m}$. XPS surveys were initially conducted, followed by high resolution XPS scans on the elements found on the

surface. Although X-rays penetrate to a depth of several micrometres, ejected photoelectrons generally come from only the first several nanometres of material making the analysis of the passive film and bulk substrate possible. In order to assess the variation in composition and to mitigate any contamination effects each sample was subjected to an argon-ion etch at $1\mu\text{A}/3\text{mm}^2$. Using licensed CasaXPS fitting software, the height, area and position of the peaks was determined allowing the separation of measured XPS spectra. The binding energy scale was calibrated for the C-1s electrons at 284.5eV. All the results in this paper use the standard format and units (CPS versus BE). Elemental concentrations are given in atomic percentages normalised to 100at% after background removal using Shirley background subtraction. Values of binding energies, FWHM and relative sensitivity factors were taken from literature and applied to the data received (Fairley et al., 2009; Hodgson et al., 2004; Kocija et al., 2004; Milosiev and Remskar, 2009; Ouerd et al., 2008).

Fourier transform infrared spectroscopy (FT-IR) analysis was also conducted in order to ascertain the current nature of any organic material present on the surfaces of the retrieved components. FT-IR scans were conducted from a wavelength of $600\text{-}5000\text{cm}^{-1}$. Reference spectra were taken from the Sigma library of FT-IR spectra and cross compared with the obtained spectra (Keller, 1986).

3. Results

3.1. Unworn, un-cemented Ultima TPS femoral stem

Figure 4a demonstrates the light field image of the Pt-CoCrMo interface and bulk alloy with the associated areas in which diffraction analysis was conducted for an unworn, uncemented Ultima TPS femoral stem. Re-crystallisation of the material had occurred within the top 200nm of the alloy, with crystals appearing to be finer, thought to results from manufacturing processes. Figure 4b demonstrates dark-field image at the Pt-CoCrMo interface. In dark field imaging, only the light scattered by crystals just off the Bragg conditions for diffraction are observed. This offers a difference in contrast which will help differentiate nano-crystalline structures. The crystals orientated to give Bragg diffraction in the nano-crystalline layer are usually characterised by finer and brighter spots of light whilst single crystal structures are usually characterised by uniform bright patches.

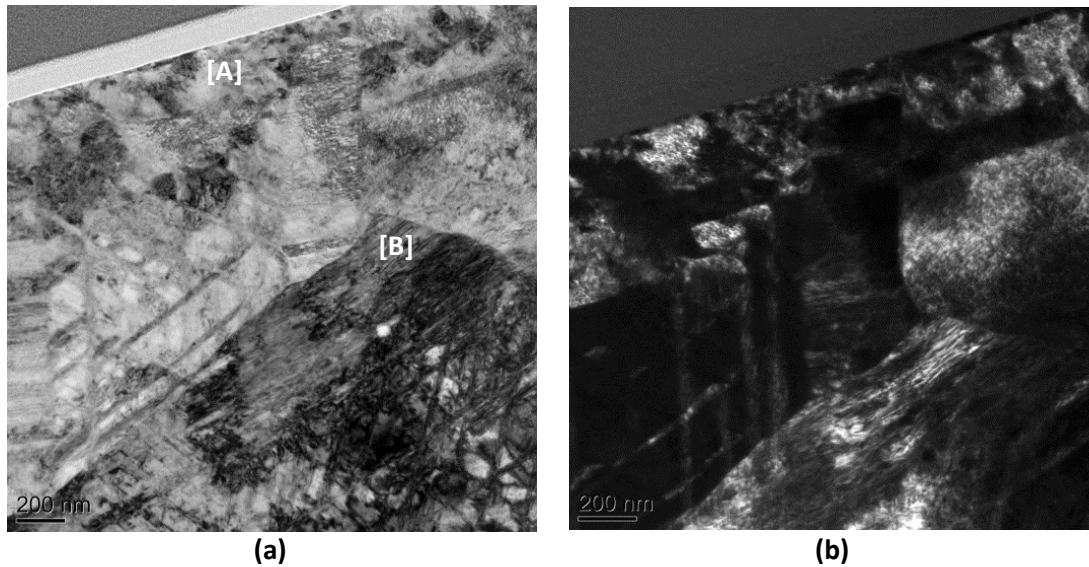


Figure 4 - a) Light field and b) dark field TEM imaging of virgin polished CoCrMo surfaces

For added clarity Selected Area Electron Diffraction (SAED) patterns were examined at different subsurface locations (Figure 5) The diffraction patterns that were observed in the upper most regions of the surface further supported the images in Figure 5, demonstrating a fine nano-crystalline layer typically characterised by the ringed diffraction pattern presented in Figure 5. Indexing of this diffraction pattern demonstrated a d-spacing characteristic of ϵ -cobalt demonstrating a hexagonal packing structure. The diffraction pattern presented in Figure 5b suggests a single crystal with a diameter greater in length than the 300nm microscope aperture. This was indexed against a cubic structure.

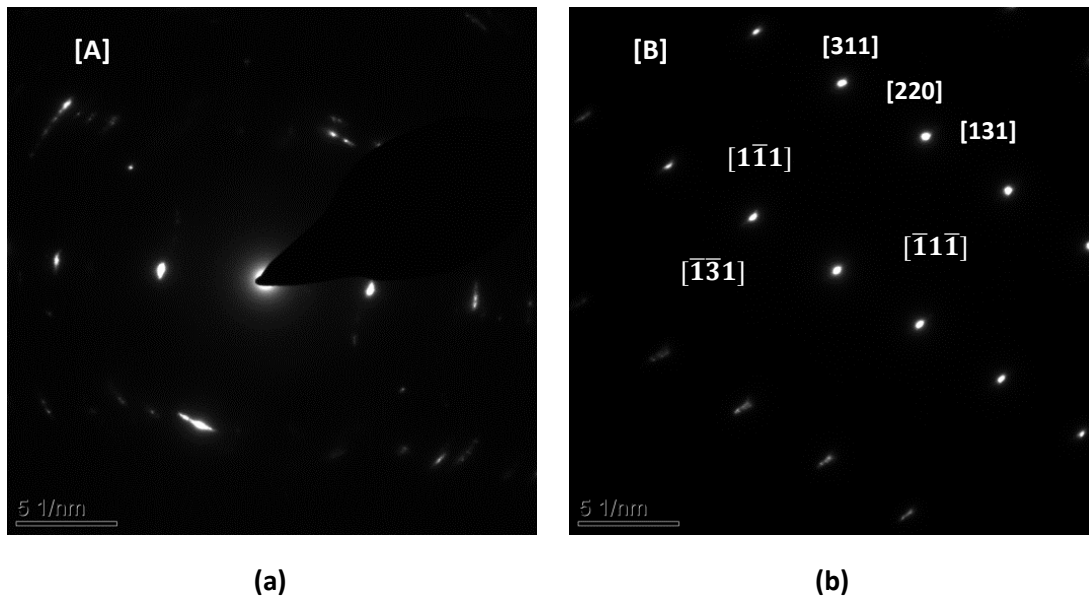


Figure 5 - SAED Patterns taken from region a) [A] and b) [B]

Further inspection with the TEM demonstrated the presence of an amorphous seeming interface or layer in the region of 2-3nm at the metal-Pt interface (Figure 6). Line EDX analysis was adopted in an attempt to quantify this interfacial layer (Figure 7). From EDX analysis C, Pt, Cu were mainly seen within the interfacial layer. Increasing amounts of Co, Cr and O were also seen with increasing scan length with yellow peaking right at the interface (approx 0.011 μ m). It still remains unclear if this is the native Cr₂O₃ oxide film or a result of carbon contamination. It is interesting to see a gradient of species in the upper most surface of the CoCrMo, with the main alloying constituents being seen to become constant at a scan length > 0.015 μ m. This corresponds to an approximate depth of the surface of 4.2nm. Co was seen to become constant at surface depth of 12.30nm. All elements were seen to remain constant after this point.

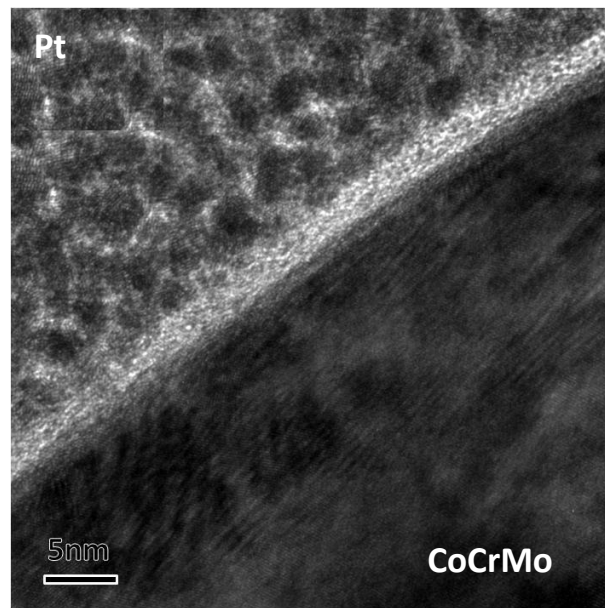


Figure 6 – Interface found at the metallic-Pt interface of an unworn Ultima TPS femoral stem

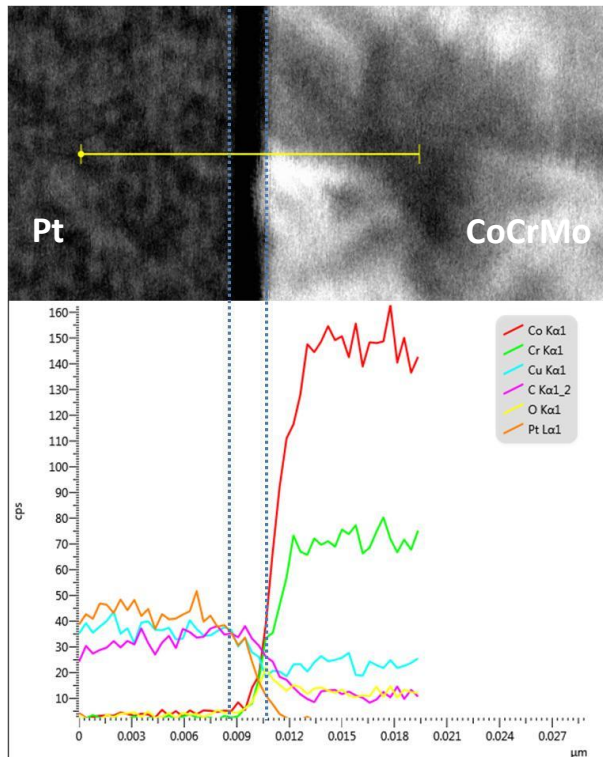
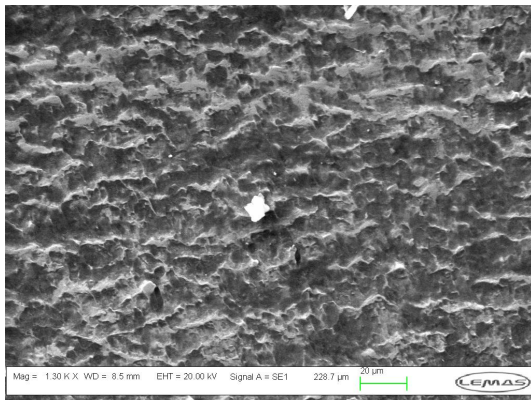


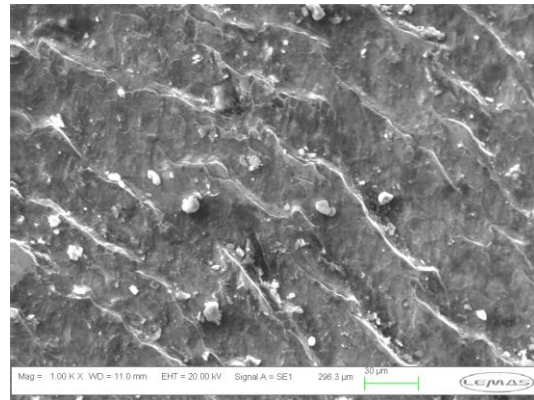
Figure 7 – Line EDX analysis of metal-Pt interface seen on the new unworn Ultima TPS femoral stem surface

3.2. Retrieved Ultima TPS femoral stems

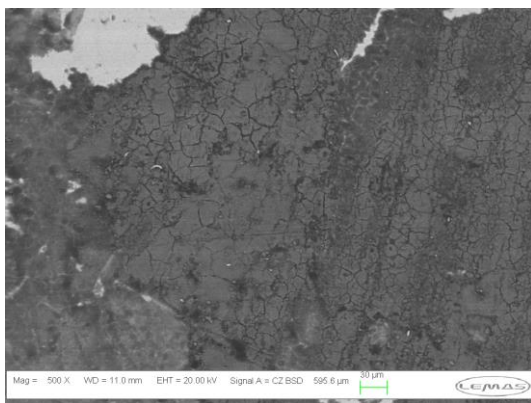
SEM/EDX analysis was conducted on sectioned femoral stems in order to fully characterise the surface morphology of retrieved femoral stems, in an attempt to understand the mechanisms of failure (Figure 8). At high magnification, clear ploughing and plastic deformation of the surface could be seen, with retention of debris within the valleys of the troughs (Figure 8a-b). Spot EDX analysis was conducted on the debris seen in Figure 8b, suggesting that the debris was Cr, O and C rich. However it is not known if this is fragmented PMMA bone cement with a Cr_2O_3 transfer film or Cr_2O_3 resulting from fretting corrosion at the interface. Attack which had characteristics of a more corrosive attack, in the absence of any micro-motion, was seen towards the distal regions of the retrieved femoral stems.



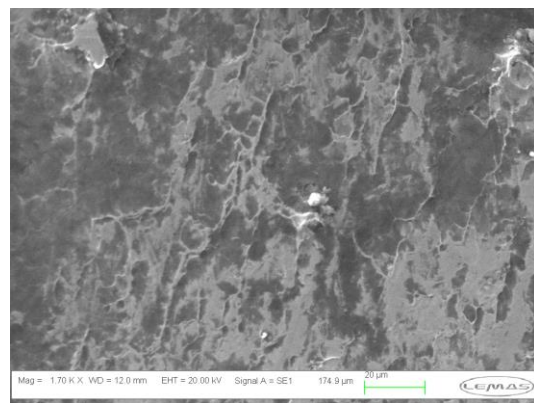
(a)



(b)



(c)



(d)

Figure 8 – SEM images of (a) plastically deformed surfaces in Gruen Zone 7 (b) surface morphology in Gruen zone 2 demonstrating the retention of debris within the grooves valleys of the plastically deformed surfaces (c) areas of black deposit seen in Gruen zone 2 and 6. Note the crazy paving like structure of the film on the surface (d) corrosion attack in Gruen zone 4. Note the loss of material in the absence of any indication of directionality on the surface.

The deposited layers were also observed using the ESEM. These were seen to comprise of smooth plaques with an irregular size and shape as shown in Figure 8c. The areas with surface deposits demonstrated a semi-conductive nature, suggesting build-up of a non-conducting film. EDX mapping was further utilised, demonstrating that the surface deposit was rich in Cr, O and N (Figure 9). Traces of Co, and Mo were also seen to be present in the surface deposit though not in the same quantities observed in the clean bulk material.

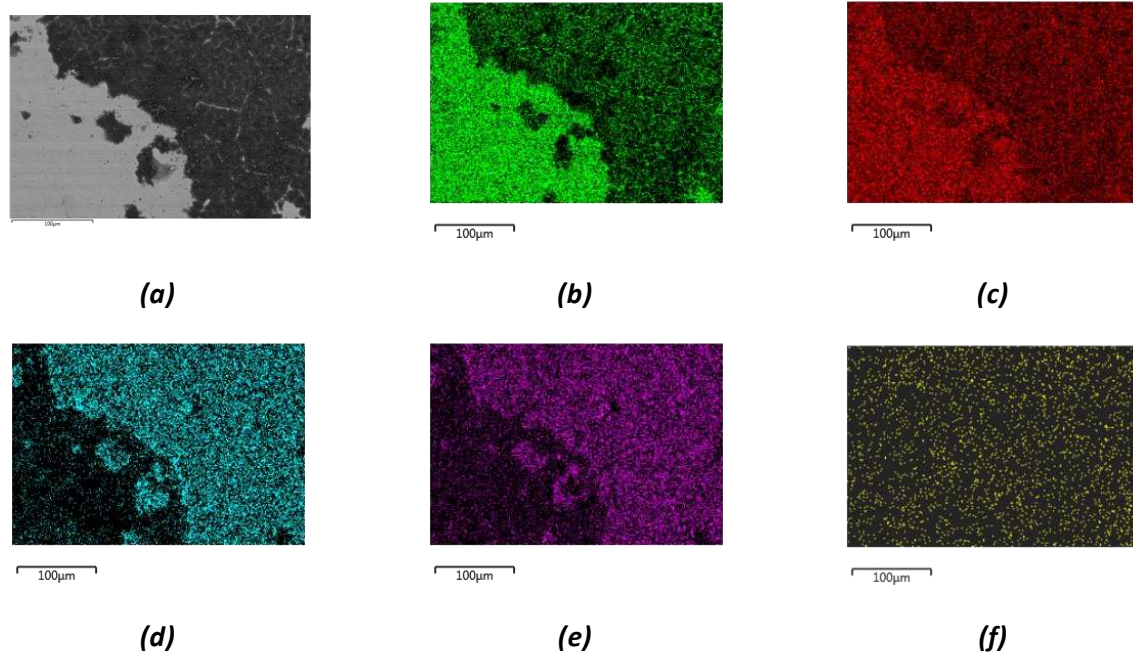


Figure 9 – EDX mapping of (a) Electron image (b) Co (c) Cr (d) C (e) O (f) N the deposit commonly seen on femoral stems demonstrating moderate to high fretting-corrosion grading.

FIB/SEM preparation techniques, along with TEM and EDX analysis proved a useful tool when identifying the exact morphology and chemistry of the deposits found on top of the retrieved femoral stems. Figure 10a illustrates the thickness and morphology of the film found on the surface of the retrieved femoral stems under TEM conditions. A thick surface film, in the region of $1\mu\text{m}$, was seen on the surface of the retrieved metallic femoral stem in the regions of high fretting-corrosion. It is interesting to note the heterogeneous nature of the film present on the surface which contains large voids surrounded by densely packed nano-sized particles. At higher magnifications, TEM analysis indicated that the particles found in surface film commonly consisted of two seemingly ellipsoid shapes joined together, surrounded by an organic amorphous matrix (Figure 10b). Figure 10c shows a selected area electron diffraction pattern taken from the surface film. Analysis of the diffraction pattern indicated the presence of Cr_2O_3 particles within the deposited layer. The interface between the metallic stem and deposit found on the femoral component was also analysed in order to assess whether any localised chemical or crystalline reorientation had occurred due to chemical dissolution or mechanical wear. At higher magnification, the metallic surface showed signs of a ‘saw tooth’ like morphology (Figure 10d), a result of fretting-corrosion. Although TEM analysis demonstrated the presence of stacking faults and annealing twins, no localised

reorientation of the metallic lattice was observed for samples that had been subjected to wear and corrosion. This due to the nature and magnitude of the slip mechanism and magnitude of shear stresses acting at the metallic interface [20].

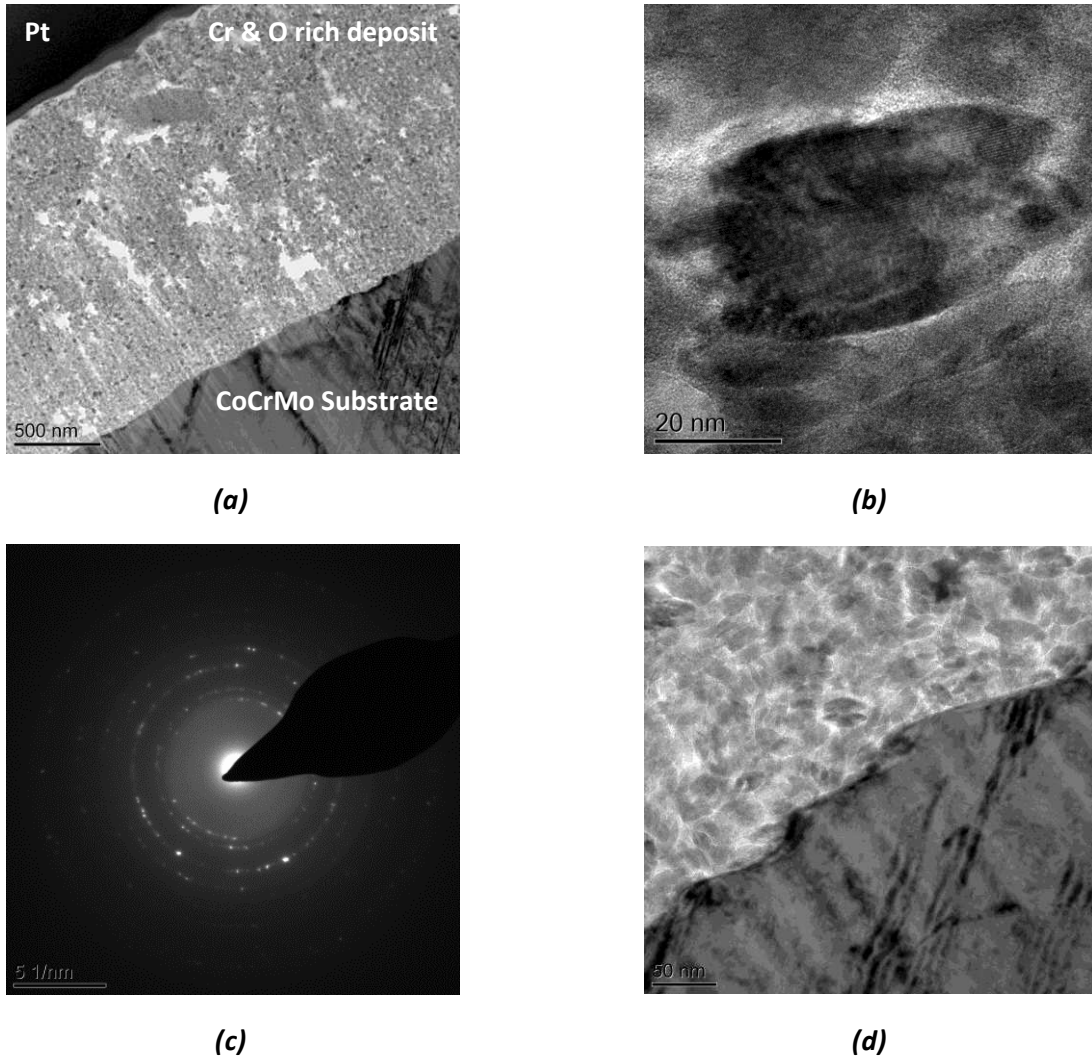


Figure 10 – Cross-sectional TEM images of (a) black deposit seen on retrieved femoral stems (b) Cr₂O₃ particles seen within the surface deposit (c) annotated diffraction pattern associated with the Cr₂O₃ film and (d) the metal-deposit interface. No localised re-orientation of the CoCrMo crystalline structure was seen.

Scanning (S)TEM/EDX mapping of the substrate and surface film was utilised in order to identify the chemical composition of the surface film. Figure 11 shows the EDX maps that were obtained for the

retrieved sample with the surface film present. It is interesting to note that the film present on the femoral stems mainly consisted of Cr, O and trace amounts of C whilst Mo was seen to be relatively well dispersed within film and the underlying material (although the generally weak signal in the Mo map makes it difficult to accurately assess its dispersion). However a clear and distinct difference in Co content at the interface between the film that had formed and the metallic substrate was seen. Co was not seen to be present in the surface film formed in-vivo.

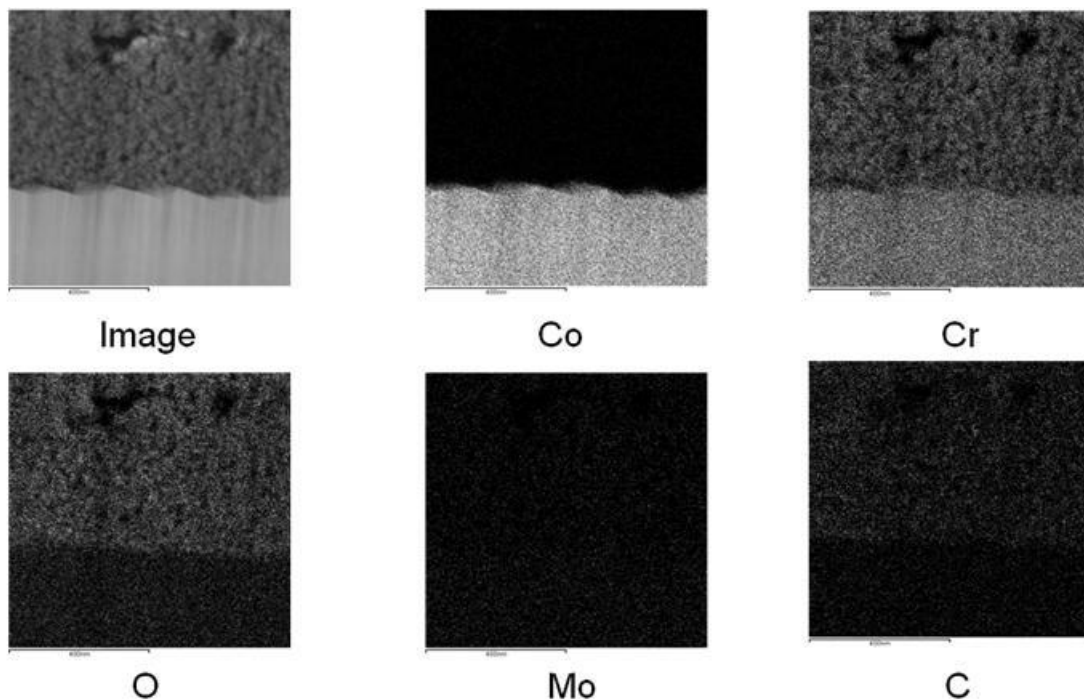


Figure 11 - TEM/EDX mapping of the substrate and deposited film. EDX analysis indicated the surface deposit was rich in Cr, O. Traces of C were also seen in the surface deposit.

XPS was further utilised in order to investigate the exact chemical composition of the surface film. After the initial surface etch had been applied, general surface scans were conducted on areas clean and free from fretting-corrosion or deposited layers and areas demonstrating the deposited layer. Figure 12 demonstrates the survey spectra that were recorded from a clean and soiled area of a retrieved Ultima TPS femoral stem with the related chemical compositions in Table 1. C, O and N were present at both sites. However an increase in C, O, N and Ca was seen in the areas of deposit. Decreases in the atomic percentage (at%) of metallic elements (Fe, Co, Cr, Mo) were seen with the areas of surface deposits.

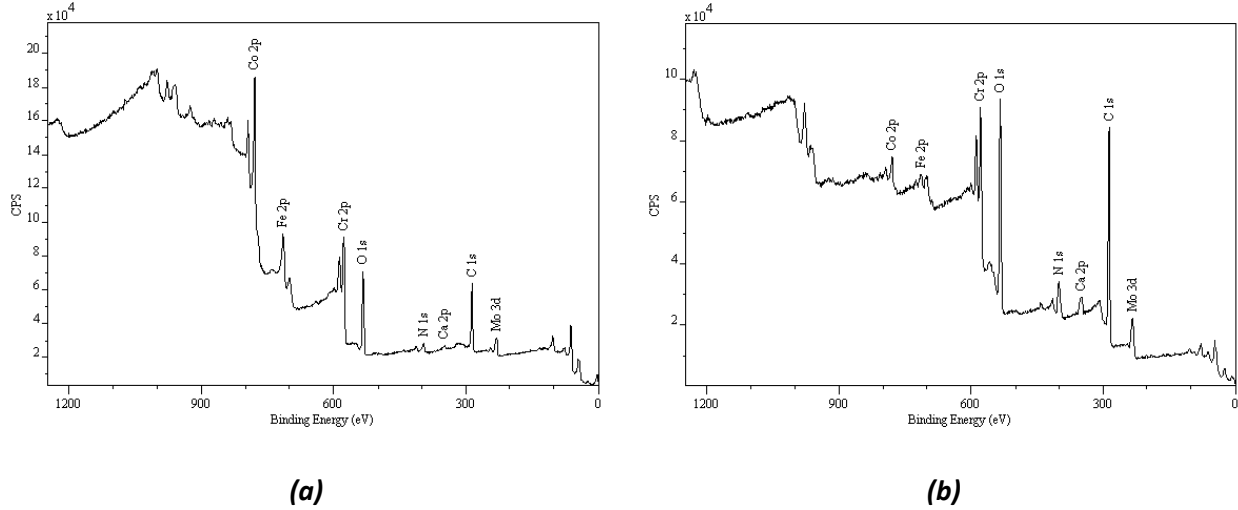


Figure 12 – General XPS survey spectra obtained for the (a) clean (b) deposited areas

Table 1 – Obtained chemical composition from XPS analysis of (a) clean and (b) deposited areas

Name	Peak Position (eV)	at %	Name	Peak Position (eV)	at %
C 1s	284.52	60.79	C 1s	284.91	66.76
Ca 2p	347.22	0.96	Ca 2p	347.31	1.58
Co 2p	778.02	5.37	Co 2p	777.91	1.07
Cr 2p	574.12	6.94	Cr 2p	576.22	4.45
Fe 2p	712.82	2.71	Fe 2p	229.32	0.99
Mo 3d	227.42	1.48	Mo 3d	398.82	6.99
N 1s	398.51	7.41	N 1s	530.62	18.16
O 1s	530.52	14.32	O 1s	284.91	66.76

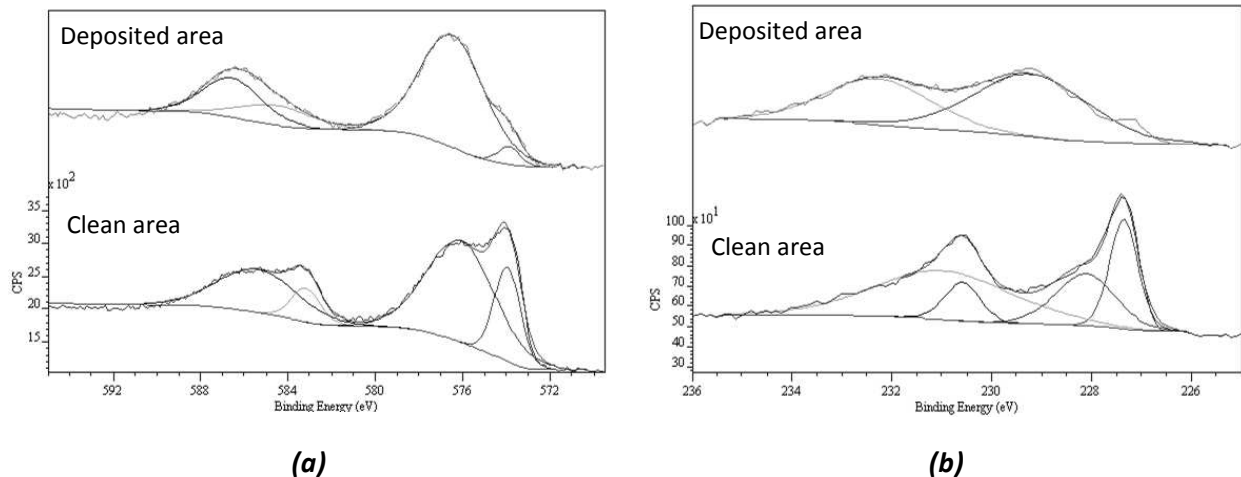
(a) Clean area

(b) Deposited areas

The advantage of XPS analysis is the possibility to identify the oxidation state and chemical environment of a particular element. Discrete differences were seen in the high resolution scans demonstrating a difference in the chemical nature of the surfaces. High resolution XPS analysis of the different areas demonstrated subtle difference in chemical state of deposited and clean areas. Although an increase in at% of elements was seen between the area free from and containing

deposit, no difference in the chemical speciation was seen for Co, Ca and O. Differences in chemical state were seen for Cr, Mo, N and C. Figure 13 demonstrates the high resolution Cr, Mo, N and C XPS spectra obtained for both the clean and areas containing the deposit.

Curve fitting of the high resolution Cr 2p spectrum demonstrated that metallic Cr and Cr₂O₃ was seen in both areas with peaks being resolved at 573.98 and 583.188eV and 576.06 and 585.36eV respectively. However the intensity of the peaks were seen to change depending on the area analysed, with deposited areas demonstrating an intense peak of Cr₂O₃ peaks when compared to the clean areas which presented dominant Cr metal peaks. A difference in Mo spectrum was also seen. For the spectra obtained from clean unworn areas, peaks were obtained at 227.35 and 230.99eV and 228.11 and 230.58eV demonstrating the presence of metallic Mo₂C and Mo respectively. For the deposited area, peaks were only observed, at relatively low intensity, at 229.20 and 232.27eV indicating the presence of MoO₂. Traces of N were seen in both areas of the analysis. In each case, peaks were resolved at 395.25 and 399.19eV demonstrating the presence of nitride and organic N. An increase in organic N was seen in deposited areas demonstrating that the film formed on the surface is a complex mixture of organic and metallic materials. Differences were also seen in the carbon spectra, with peaks being resolved at 284.88 and 286.27eV suggesting elemental C and C with N. An addition peak was seen on the C 1s spectra indicating the presence of carbides, likely to M₇C₃.



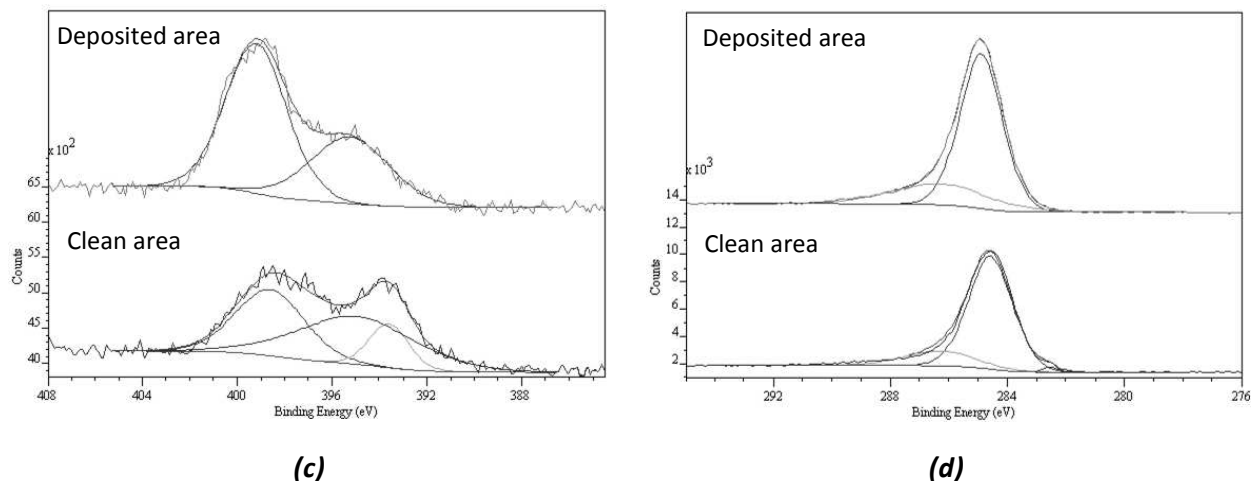
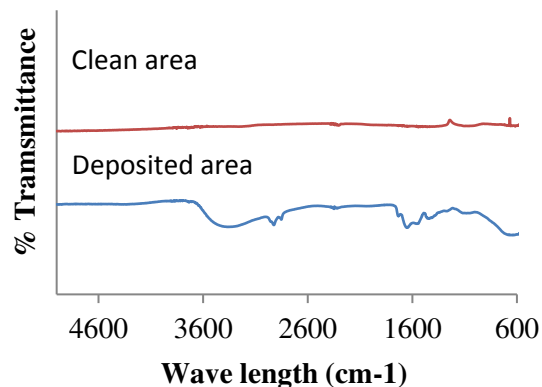


Figure 13 – Curve fitted, high resolution XPS spectra obtained for (a) Cr 2p (b) Mo 3d (c) N 1s and (d) C 1s

FT-IR was utilised in order to determine the chemical structure and bonds present on the surface of the retrieved samples. FT-IR analysis was again conducted on the deposited layer and clean areas of retrievals. Figure 14 demonstrates the FT-IR spectra obtained from the retrieved cohort. FT-IR demonstrated that no chemical bonds were present on the surface of the clean metallic area. FT-IR analysis on the deposited areas demonstrated characteristics of human serum albumin suggesting that no unfolding or denaturing of the proteins had occurred on the surface, although the film seemed to be mechanically mixed with Cr_2O_3 debris.



Peak Location (cm^{-1})	Class	Structure
3384	Alkanes	$\text{RCH}_2\text{2CH}_3$
2932	Carboxylic acid	RCO-OH
2860	Carboxylic acid	RCO-OH
2252		C-N
2062		C=N
1740	Amide	C=O
1662		C=N
1574	Carboxylic	C-O
1458	Alkanes	$\text{CH}_2 \text{CH}_3$
1130	Phosphate	P=O
668	Alkynes	C-H

(a)

(b)

Figure 14- (a) FT-IR analysis of clean and deposited areas with (b) associated peak locations and structures seen on clean and deposited areas.

4. Discussion

To date, the occurrence of fretting-corrosion at the stem-cement interface has been extensively reported as a source of wear and PMMA particle debris in clinical studies, being shown to elicit loosening of femoral component and osteolysis. However the exact tribo-chemical and tribological interactions taking place at these interfaces are not well investigated. Fretting-corrosion has been observed in a number of clinical cases on both polished and matte femoral stems (Burston et al., 2012; Fowler et al., 2011; Gie and Ling, 1994; Jasty et al., 1991). Howell et al (Howell et al., 2004) presented a comprehensive study, conducting SEM and 3-D interferometry analysis on both retrieved polished and matte femoral stems, identifying that polished and matte femoral stems present two very different wear mechanisms. Polished stems were seen to exhibit signs of ductile wear accompanied by pitting of the surface, a similar morphology observed in this cohort, whilst matte stems presented evidence of abrasive or truncation wear. Blunt et al (Blunt et al., 2009) and Zhang et al (Zhang et al., 2011; Zhang et al., 2009; Zhang et al., 2012; Zhang et al., 2013) have also contributed to the area by characterising the surface morphology and some of the mechanisms leading to the initiation and propagation of fretting wear on stainless steel femoral stems. However, at the present, no studies have quantified the tribochemical reactions occurring within the stem-cement interface and the influence these have on the overall degradation and chemistry of debris released into the biological environment.

4.1. Previous studies on tribo-films

The importance of tribo-chemistry in orthopaedics was first recognised by Wimmer (Wimmer et al., 2003), who highlighted the role proteins play at the bearing interfaces. It was demonstrated that tribochemical layers for retrieved MoM bearings consisted of organic proteins and constituents of salts, with a good correlation between retrieved and in-vitro analysis. It was further hypothesised that these films reduced the amount of wear due by serving as a type of transient solid lubricant. The presence of protein-containing tribo-films has also been shown to result in reduction of wear enhanced-corrosion. Yan et al (Yan et al., 2009) demonstrated that proteins can influence the rates of both wear and corrosion by interacting with metallic ions and forming complex films within the tribological contact resulting in 'wear-induced passivation' of the surface. Other reports investigating films formed on retrieved bearing surfaces have identified subtly different changes in film chemistry with respect to the thickness of the film. Milošev (Milosiev and Remskar, 2009) identified that thick deposits were commonly due to denature proteins, being predominantly C, N

and O rich whilst thinner films were often a complex mix of organic material, metal oxides and hydroxides. A recent study by Liao et al (Liao et al., 2011) further suggested that these films may be graphitic providing enhanced lubrication properties. It was noted that such layers are not simply formed due to the sheer stresses and contact pressures experienced *in-vivo*, but possibly due to catalytic reactions initiated by the presence of metallic elements resulting in the elimination of water and ammonia from organic materials. Although the majority of studies to date demonstrate and characterise the complex tribo-chemical reactions taking place at the articulation surface, this study is one of a few to utilise advanced surface microscopy and surface chemistry analytical techniques in order to understand the tribo-corrosion and tribo-chemical interactions at the stem-cement interface.

Walczak et al (Walczak et al., 1998) observed the surface chemistry and surface morphology of deposits found on stainless steel Charnley and Müller prostheses and also retrieved PMMA bone cement. They proposed that a multilayer film existed on the surface with different elemental chemistry. An initial Cr-rich layer was seen on the surface of the sample, accompanied by an iron rich plaque and a third chloride/sulphur plaque; however provided no cross-sectional evidence to support this. They also observed that the debris found on the surface of the retrieved PMMA bone cement had a similar chemical composition to the deposits found on the retrieved femoral components. Although this study has demonstrated a surface deposit present on the surface of the samples; TEM/EDX analysis did not demonstrate a multi-layered deposit. A film consisting of Cr_2O_3 crystallites, seemingly compressed and bound together by an amorphous organic material existed on the surface of the CoCrMo femoral stems. Diffraction patterns of the debris on the surface of the CoCrMo femoral stems demonstrated a hexagonal close packed arrangement with a d-spacing associated with Cr_2O_3 . FT-IR further demonstrated chemical bonds associated with the Human Serum Albumin protein commonly found within synovial fluid. Further supporting the fact that these films were metallic crystallites surrounded by amorphous organic material and no evidence of catalysis resulting in the elimination of water or ammonium from the protein. These observations suggest that the mechanisms under which these films are formed (i.e. at the articulation, modular taper or stem-cement interface) drastically influence the morphology and chemistry of the film formed, dependant on the levels of loading, displacement and sheer stress experienced by the metallic surface. Such factors will control the way proteins will orientate and interact with the metallic surface. In a previous *in-vitro* study (Bryant et al., 2013b), comparable tribo-films were

seen to form on both the femoral stem as well as the counterpart bone cement. Although these studies were conducted in the absence of proteins, particle morphology and film chemistries were consistent with the retrieval products (compacted crystalline metallic Cr_2O_3 debris in the absence of the surrounding organic debris).

4.2. Influence of fretting corrosion on local environment

Observations presented in this study, along with examination of the current literature relating to tribo-chemistry in THR's, raises further questions with respect to the influence of fretting-corrosion product on the surrounding biological environment. TEM imagery demonstrated the formation of thick Cr_2O_3 rich film could be seen on the CoCrMo femoral stem and counterpart PMMA bone cement. This supports the findings and hypothesis presented by Hart et al (Hart et al., 2012) who demonstrated that retrieved tissues from the Norwich cohort were Co rich, whilst patients that had been revised due to failure of a resurfacing device were seen to be Cr rich. High levels of Co can be explained by the thermodynamic stability of the species. Thermodynamics can be used to evaluate the theoretical activity of a given metal or alloy in a known corrosion environment (Revie, 2000). It is thought that Cr is favoured as the species to undergo reaction due to the lower activation energy required for oxidation resulting in the formation of Cr_2O_3 corrosion product on the metallic femoral stem and counterpart bone cement. This leaves the cobalt (Co^{2+}), known to be extremely soluble at the electrode potential and pH found at the interface, to migrate and leave the interface due to an electrical potential established across the interface due to the separation of anodic and cathodic areas. This has also been observed in experimental simulations complimenting clinical literature (Bryant et al., 2013a; Bryant et al., 2013b).

The interactions between fretting and corrosion have been well documented since the 1950's (Feng and Barrans, 1956). Fretting-corrosion occurs when two materials under load are subject to minute relative motion within an aqueous environment. The contact between the two materials causes mechanical wear and material transfer at the surfaces. However when typically passive alloys are immersed in fluids and subjected to fretting, removal of the passive film occurs exposing the reactive metallic substrate to the aqueous environment resulting in oxidation of the metallic substrate and metallic debris. Figure 15 demonstrates schematically the fretting-corrosion process taking place at the stem-cement interface and a mechanism for formation and transfer of oxidised metallic debris from the metallic stem to the counterpart PMMA bone cement. Figure 15

schematically demonstrates the depassivation and repassivation of the CoCrMo surface over one loading cycle. At the initial stages of loading (Figure 15a) the film, substrate, counter substrate and points of contact are elastically deformed. As the load is increased, the yield point of the passive film, CoCrMo substrate and PMMA bone cement is exceeded and rupture of the oxide film occurs (Figure 15b). This results in the CoCrMo substrate being exposed to the solution resulting in oxidation of the metallic substrate along with plastic deformation of the surface. At point d, maximum load has been applied and held, the stem-cement interfaces are held together with the PMMA bone cement protecting most of the ruptured sites in the oxide film from the electrolyte. It is thought that the transfer of the metal oxide occurs when the CoCrMo and PMMA bone cement surfaces are in contact resulting in compressed Cr_2O_3 debris, a common finding in fretting systems (Feng and Barrans, 1956; Geringer et al., 2005; Waterhouse, 1972). As the load is removed the surfaces gradually become separated until the contact area is sufficiently reduced to expose the ruptured oxide film and substrate to the electrolyte resulting in the further dissolution and repassivation of the oxide film (Figure 15d-e) until the surface is sufficiently protected by the oxide film to retard further oxidation.

The formation of Cr_2O_3 layers and the selective dissolution of Co are characteristics commonly found in engineering fretting systems and clinical scenarios (Bolland et al., 2011; Donell et al., 2010; Feng and Barrans, 1956). A study by Gilbert *et al* (Gilbert et al., 1993; Gilbert and Engh, 1995; Jacobs et al., 1998) identified the formation of metallic 'inter-layer' and the selective dissolution of Co within modular head-neck connections, typically characterised by 'etching' of the CoCrMo alloy. Gilbert proposed that such surface morphologies result from mechanically-assisted crevice corrosion and cold welding between two metallic interfaces. Due to the location of the black layer and no evidence of selective leaching of Co from the alloy, it is thought that the mechanism producing metal-oxide layers and Co rich external environments are different to that proposed for the head-neck taper. Thick oxide films occurring within the stem-cement interface are thought to be a result of fretting-corrosion liberating Co^{2+} , Cr^{3+} and Mo^{2+} along with fractured oxide and metallic particulate into the interface. Cyclic loading will result in the compression of any metallic oxide and debris on the stem-cement surfaces. It is thought that the compression of debris within the interfaces, along with further oxidation/redox of any metallic debris, results in the formation of thick Cr_2O_3 rich films within the interface. Mechanical mixing of the fretting-corrosion products with organic material will also occur, similar to the mechanisms described by Willert *et al* (Willert et al.,

1996) who described fresh synovial fluid to freely enter the interface as the stem-cement surfaces became separated, resulting the films to become a mixture of Cr_2O_3 and organic material.

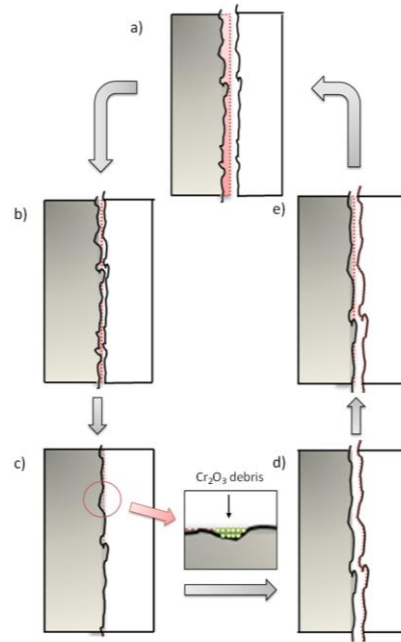


Figure 15 – Schematic representation of the fretting-corrosion process taking place at the stem-cement interface and a mechanism for metallic debris from the metallic stem to the counterpart (Bryant et al., 2013d)

It is evident from this work and review of the literature that the type of degradation mechanism can influence the type and quantities of metal ions released from the interfaces. This is supported by the experimental results presented by Wimmer (Wimmer et al., 2003), Liao (Liao et al., 2013; Liao et al., 2011), Yan (Yan et al., 2009), Hesketh (Hesketh et al., 2013) and Heisel et al (Heisel et al., 2008) who have all demonstrated that such films can reduce wear and corrosion, along with a stoichiometric release of metallic ions into the bulk environment. The formation of tribo-films within the articulation is thought to be beneficial due to the ‘wear-induced passivation’ of the surfaces reducing the rates of oxidation and improving lubrication. *In-vitro* testing of the stem-cement interface has demonstrated that Co can account for up to 95% of all metal ions released, demonstrating that the wear mechanism can drastically influence the biological environment further supporting Hart’s (Hart et al., 2012) observations. Although this and previous studies have demonstrated the formation of films within the

stem-cement interface, the true extent and implications of these films is still unknown. Hart hypothesised that Co may be the clinical relevant active species that is responsible unexplained failure of MoM THR's.

It is also interesting to note that such failure seems to occur in MoM systems when a polished CoCrMo femoral stem is used. Shetty et al (Shetty et al., 2005) presented the findings of the Ultima TPS femoral stem when used in conjunction with a MoP articulation. No hips required revision within 5 years due to ARMD. When used in conjunction with a MoP articulation the Ulitma TPS was seen to have a similar performance as the Exeter femoral stem which has at least 20 years of clinical prevalence (Shetty et al., 2006). Polished tapered femoral stems generally have a good survivorship with revision rates of 2.8% at 7 years after operation being seen for commonly cemented stainless steel devices (Fowler et al., 2011). Similar figures have been presented for CoCrMo polished demonstrating revision rates of 4.1% 10 years postoperative (Burston et al., 2012). Although anecdotal at this time, a link between high revision rates due to ARMD and high levels of wear and corrosion of polished CoCrMo femoral stems when used with an all metal bearing seems to exist (Bolland et al., 2011; Donell et al., 2010).

5. Conclusions

Advanced surface microscopy techniques combined with chemical analysis have been used to identify the surface morphology and composition of retrieved femoral components revised due to high levels of fretting-corrosion. Distinct directionality and plastic deformation of the metallic surfaces was seen, characteristic of fretting- crevice corrosion demonstrating that complex fretting, electrochemical and tribo-chemical reactions exist at the stem-cement interfaces. The formation of thick deposited layers was also seen to occur within these interfaces, with films being seen to consist of Cr_2O_3 bound with organic materials. This study has also highlighted that fretting-corrosion at the stem-cement interface can contribute to high levels of metal ions resulting in extensive soft tissue necrosis with the associated tribo-corrosion and tribo-chemical mechanism proposed.

6. References

- Blunt, L.A., Zhang, H., Barrans, S.M., Jiang, X., Brown, L.T., 2009. What results in fretting wear on polished femoral stems. *Tribology International* 42, 1605-1614.
- Bolland, B., Culliford, D., Langton, D., Millington, J., Arden, N., Latham, J., 2011. High Failure rates with a large-diameter hybrid metal-on-metal total hip replacement. *Journal of Bone and Joint Surgery [Br]* 93, 608-615.
- Bryant, M., Farrar, R., Brummitt, K., Freeman, R., Neville, A., 2013a. Fretting corrosion of fully cemented polished collarless tapered stems: The influence of PMMA bone cement. *Wear* 301, 290-299.

Bryant, M., Farrar, R., Freeman, R., Brummitt, K., Neville, A., 2013b. Fretting corrosion characteristics of polished collarless tapered stems in a simulated biological environment. *Tribology International* 65, 105-112.

Bryant, M., Ward, M., Farrar, R., Freeman, R., Brummitt, K., Nolan, J., Neville, A., 2013c. Failure analysis of cemented metal-on-metal total hip replacements from a single centre cohort. *Wear* 301, 226-233.

Bryant, M., Ward, M., Farrar, R., Freeman, R., Brummitt, K., Nolan, J., Neville, A., 2013d. Failure analysis of cemented metal-on-metal total hip replacements from a single centre cohort. *Wear* 301, 226-233.

Burston, J., Barnett, J., Amirfeyz, R., Yates, R., Bannister, G., 2012. Clinical and radiological results of the collarless polished tapered stem at 15 years follow-up. *The Journal of Bone and Joint Surgery [Br]* 94.

Donell, S., Darrah, C., Nolan, J., Wimhurst, J., Toms, A., Barker, T., Case, C., Tucker, J., 2010. Early failure of the Ultima metal – on – metal total hip replacement in the presence of normal plain radiographs. *Journal of bone and joint surgery [Br]* 92, 1501-1508.

Fairley, N., Ltd, C.S., Ltd, C.S., 2009. CasaXPS Manual 2.3.15: Introduction to XPS and AES. Casa Software, Limited.

Feng, I., Barrans, S., 1956. An experimental study of fretting. *Proceedings of the Institution of Mechanical Engineers* 170, 1055-1064.

Fowler, J., Gie, G., Lee, A., Ling, R., 2011. Experience with the Exeter total hip replacement since 1970. *Orthopaedic clinics of North America* 19.

Geringer, J., Forest, B., Combrade, P., 2005. Fretting-corrosion of materials used as orthopaedic implants. *Wear*, 943-951.

Gie, G., Ling, R., 1994. Loosening and the Migration of the Exeter THR. *The Journal of Bone and Joint Surgery [Br]* 76.

Gilbert, J., Buckley, C., Jacobs, J., 1993. In vivo corrosion of modular hip prosthesis components in mixed and similar metal combinations. The effect of crevice, stress, motion, and alloy coupling. *Journal of Biomedical Materials Research* 27, 1533-1544.

Gilbert, J., Engh, C., 1995. *Mechanical -electrochemical interactions occurring during in vitro fretting corrosion tests of modular connection*. Total hip revision surgery, 41-50.

Gruen, T., McNeice, G., Amustuz, H., 2011. Modes of Failure of Cemented Stem-type Femoral Components: A radiographic analysis of Loosening. *Clin Orthop Relat Res*.

Hart, A.J., Quinn, P.D., Lali, F., Sampson, B., Skinner, J.A., Powell, J.J., Nolan, J., Tucker, K., Donell, S., Flanagan, A., Mosselmans, J.F.W., 2012. Cobalt from metal-on-metal hip replacements may be the clinically relevant active agent responsible for periprosthetic tissue reactions. *Acta Biomaterialia* 8, 3865-3873.

Heisel, C., Striech, N., Krachler, M., Jaubowitz, E., Kretzer, P., 2008. Characterization of the running-in period in total hip resurfacing arthroplasty: An in vivo and in vitro metal ion analysis. *J Bone Joint Surg Am* 90, 125-133.

Hesketh, J., M, Q., Dowson, D., Neville, A., 2013. Biotribocorrosion of metal-on-metal hip replacements: How surface degradation can influence metal ion formation. *Tribology International*.

Hodgson, A., Kurz, S., Virtanen, S., Fervel, V., Olsson, C., Mischler, S., 2004. Passive and transpassive behaviour of CoCrMo in simulated biological solutions. *Electrochimica Acta* 49, 2167-2178.

Howell, J.R., Blunt, L.A., Doyle, C., Hooper, R.M., Lee, A.J.C., Ling, R.S.M., 2004. In Vivo surface wear mechanisms of femoral components of cemented total hip arthroplasties: the influence of wear mechanism on clinical outcome. *The Journal of Arthroplasty* 19, 88-101.

Jacobs, J., Gilbert, J., Urban, R., 1998. *Current concepts review – Corrosion of metal orthopaedic implants*. *The Journal of Bone and Joint Surgery* 80, 268-282.

Jasty, M., Maloney, W., Bragdon, C., O'Conner, D., Haire, T., Harris, W., 1991. The initiation of failure in cemented femoral components of hip arthroplasties. *The Journal of Bone and Joint Surgery [Br]* 73-B, 551-558.

Keller, R.J., 1986. The Sigma library of FT-IR Spectra, 1 ed. Sigma chemical company, St Louis, USA.

Kocija, A., Milosev, I., Pihlar, B., 2004. Colbalt-based alloys for orthopeadic applications studied by electrochemical and XPS analysis. *Journal of Materials Science: Materials in Medicine* 15, 643-650.

Liao, Y., Hoffman, E., Wimmer, M.A., Fischer, A., Jacobs, J.J., Marks, L.D., 2013. CoCrMo Metal-on-metal hip replacements. *Phys.Chem.Chem.Phys.* 15, 746-756.

Liao, Y., Pourzal, R., Wimmer, M.A., Jacobs, J.J., Fischer, A., Marks, L.D., 2011. Graphitic Tribological Layers in Metal-on-Metal Hip Replacements. *Science* 334, 1687-1690.

Milosiev, I., Remskar, M., 2009. In vivo production of nanosized metal wear debris formed by tribochemical reaction as confirmed by high-resolution TEM and XPS analyses. *Journal of Biomedical Materials Research Part A* 91A, 1100-1110.

Mischler, S., 2003. Electrochemical control of wear: a third body approach, in: D. Dowson, M.P.G.D., Lubrecht, A.A. (Eds.), *Tribology Series*. Elsevier, pp. 47-56.

Muratov, V., Luangvaranunt, T., Fischer, T., 1998. The Tribochemistry of silicon nitride: effects of friction, temperature and sliding velocity. *Tribology International* 31, 601-611.

National Joint Registry, 2012. National Joint Registry for England and Wales: 9th Annual Report 2012, <http://www.njrcentre.org.uk/NjrCentre/LinkClick.aspx?fileticket=QkPI7kk6B2E%3d&tabid=86&mid=52>.

Ouerd, A., Alemany-Dumony, C., Normand, B., Szunerits, S., 2008. Reactivity of CoCrMo alloy in physiological medium: Electrochemical characterization of the metal/protein interface. *Electrochimica Acta* 53, 4461-4469.

Revie, R., 2000. *Thermodynamics: corrosion tendency and electrode potentials, Corrosion and corrosion control*, 1 ed. John Wiley and Sons, New York, pp. 22-66.

Reynolds, L.A., Tansey, E.M., 2006. EARLY DEVELOPMENT OF TOTAL HIP REPLACEMENT, 1 ed. Wellcome Trust Centre, London, UK.

Shetty, N., Hamer, A., Kerry, R., Stockley, I., Eastell, R., Wilkinson, J., 2006. Exeter versus Ultima-TPS femoral stem: a randomised early outcomes study. *The Journal of Bone and Joint Surgery [Br]* 88-B.

Shetty, N., Hamer, A., Stockley, I., Eastell, R., Wilkinson, J., 2005. Clinical and radiological outcome of total hip replacement five years after pamidronate therapy. *The Journal of Bone and Joint Surgery [Br]* 88-B, 889.

Walczak, J., Shahgaldi, F., Heatley, F., 1998. In vivo corrosion of 316L stainless-steel hip implants: morphology and elemental compositions of corrosion products. *Biomaterials* 19, 229-237.

Waterhouse, R.B., 1972. Fretting Corrosion. International series of monographs on materials science and technology, Pergamon press.

Willert, H., Broback, L., Buchhorn, G., Jemsen, P., Koster, K., Lang, I., Ochsner, P., Schenk, R., 1996. Crevice corrosion of cemented titanium alloy stems in total hip replacements. *Clin Orthop Relat Res* 333, 333-351.

Wimmer, M.A., Sprecher, C., Hauert, R., T+ñger, G., Fischer, A., 2003. Tribochemical reaction on metal-on-metal hip joint bearings: A comparison between in-vitro and in-vivo results. *Wear* 255, 1007-1014.

World Health Organisation, 2003. Musculoskeletal conditions affect millions, *Corrosion Science*.

Yan, Y., Neville, A., Dowson, D., Williams, S., Fisher, J., 2009. Tribofilm formation in biotribocorrosion- does it regulate ion release in metal-on-metal artificial hip joints? *Proc.IMechE Pat H: J.Engineering in Medicine* 224, 997-1005.

Zhang, H., Brown, L., Blunt, L., Jiang, X., Barrans, S., 2011. The contribution of the micropores in bone cement surface to generation of femoral stem wear in total hip replacement. *Tribology International* 44, 1476-1482.

Zhang, H., Brown, L.T., Blunt, L.A., Jiang, X., Barrans, S.M., 2009. Understanding initiation and propagation of fretting wear on the femoral stem in total hip replacement. *Wear* 266, 566-569.

Zhang, H.Y., Blunt, L.A., Jiang, X.Q., Fleming, L.T., Barrans, S.M., 2012. The influence of bone cement type on production of fretting wear on the femoral stem surface: A preliminary study. *Clinical Biomechanics* 27, 666-672.

Zhang, H.Y., Luo, J.B., Zhou, M., Zhang, Y., Huang, Y.L., 2013. Biotribological properties at the stem–cement interface lubricated with different media. *Journal of the Mechanical Behavior of Biomedical Materials* 20, 209-216.

LIST OF FIGURES

Figure 1 – A schematical representation of a THR with the associated tribo-corrosion mechanisms.

Figure 2 – Ulitma TPS™ MoM total hip replacement used in the Norwich cohort

Figure 3 – FIB SEM preparation of TEM section (a) surface prior to Pt deposition (b) electron deposited Pt layer (c) ion deposited layer (d) bulk removal of material either side of the section (e) cutting the section free prior to removal (f) removal of the section (g) fixation of FIB prepared section to Cu TEM grid and (h) final thinning of the prepared section.

Figure 4 - a) Light field and b) dark field TEM imaging of virgin polished CoCrMo surfaces

Figure 5 - SAED Patterns taken from region a) [A] and b) [B]

Figure 6 – Interface found at the metallic-Pt interface of an unworn Ultima TPS femoral stem

Figure 7 – Line EDX analysis of metal-Pt interface seen on the new unworn Ultima TPS femoral stem surface

Figure 8 – SEM images of (a) plastically deformed surfaces in Gruen Zone 7 (b) surface morphology in Gruen zone 2 demonstrating the retention of debris within the grooves valleys of the plastically deformed surfaces (c) areas of black deposit seen in Gruen zone 2 and 6. Note the crazy paving like structure of the film on the surface (d) corrosion attack in Gruen zone 4. Note the loss of material in the absence of any indication of directionality on the surface.

Figure 9 – EDX mapping of (a) Electron image (b) Co (c) Cr (d) C (e) O (f) N the deposit commonly seen on femoral stems demonstrating moderate to high fretting-corrosion grading.

Figure 10 – Cross-sectional TEM images of (a) black deposit seen on retrieved femoral stems (b) Cr₂O₃ particles seen within the surface deposit (c) annotated diffraction pattern associated with the Cr₂O₃ film and (d) the metal-deposit interface. No localised re-orientation of the CoCrMo crystalline structure was seen.

Figure 11 - TEM/EDX mapping of the substrate and deposited film. EDX analysis indicated the surface deposit was rich in Cr, O. Traces of C were also seen in the surface deposit.

Figure 12 – General XPS survey spectra obtained for the (a) clean (b) deposited areas

Figure 13 – Curve fitted, high resolution XPS spectra obtained for (a) Cr 2p (b) Mo 3d (c) N 1s and (d) C 1s

Figure 14- (a) FT-IR analysis of clean and deposited areas with (b) associated peak locations and

Figure 15 – Schematic representation of the fretting-corrosion process taking place at the stem-cement interface and a mechanism for metallic debris from the metallic stem to the counterpart (Bryant et al., 2013d)

LIST OF TABLES

Table 1 – Obtained chemical composition from XPS analysis of (a) clean and (b) deposited areas